Bulk pH Responsive DNA Quadruplex Hydrogels Prepared by Liquid-Phase Large Scale DNA Synthesis

Shizuma Tanaka,[†] Shinsuke Yukami,[†,§] Kazuki Fukushima,[†,§] Kenta Wakabayashi,[†] Yuichi Ohya,*,[†,‡] and Akinori Kuzuya*,[†,‡]

[†]Department of Chemistry and Materials Engineering, Kansai University, 3-3-35 Yamate, Suita, Osaka 564-8680, Japan.

[‡]Collaborative Research Center of Engineering, Medicine, and Pharmacology, ORDIST, Kansai University, 3-3-35 Yamate, Suita, Osaka 564-8680, Japan.

ABSTRACT: A new pH-responsive hydrogel biomaterial, that is composed of solely two popular bio-compatible materials, oligodeoxynucleotides (ODN) and polyethylene glycol (PEG) have been prepared. Merely five deoxycytidine residues were elongated to the ends of linear or 4-arm PEG in ×1000 larger scale than conventional systems by using liquid-phase DNA synthesis technique, and applied them as a macromonomer for the preparation of hydrogels. The syntheses of the conjugates are simply elongating ODN onto the ends of PEG as a semi-solid phase substrate using standard phosphoramidite chemistry. The resulting dC5-PEG conjugates gave quite stable and stiff hydrogels triggered by the formation of a unique DNA quadruplex, i-motif. Introduction of only one chemical linkage between two linear conjugates resulted in unexpectedly high thermal stabilities for the melting temperatures of i-motifs themselves. Non-linearly improved rheological properties compared to the original linear conjugates were also observed, probably because of topological entanglement between macromonomers of fused circles.
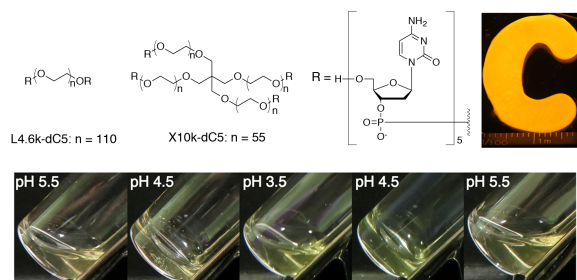
Hydrogels are attracting broad interest not only from chemistry or material science but also from various research fields related to medical science because of their potential as future drug carriers, cell culture scaffold, etc.[1] DNA is one of popular components to construct intelligent hydrogels,[2] by utilizing the fruits of eager studies in DNA computing and structural DNA nanotechnology.[3]

Not only regular duplexes,[4] four-stranded structures called G-quadruplex are often used to construct DNA hydrogels because of its attractive features such as metal ion binding capability and quite high thermal stabilities.[5,6] We as well have recently reported a new class of hydrogels utilizing G-quadruplexes as crosslinking points.[7] Oligodeoxynucleotides (ODN) -PEG conjugates bearing merely four deoxyguanosine residues (dG4) at the ends of linear or branched PEG were prepared by applying high-efficiency liquid phase (HELP) synthesis of oligonucleotides developed by Bonora *et al.* with a few major modifications.[8] This technique enables us to prepare typically ten to twenty grams of ODN-PEG conjugates in laboratories and to overcome size-barrier of popular solid-phase DNA synthesis,[9] which only produces oligonucleotides in less than milligrams. By using dG4-PEG conjugates prepared as such, intelligent, biodegradable, and self-healing hydrogels (G-quadruplex gels), which turn into gel quite rapidly upon addition of various body-related fluids such as serum, artificial sweat or tear, or even simple phosphate buffered saline (PBS), were constructed.

a)

L4.6k-dC5 = ∿

b)

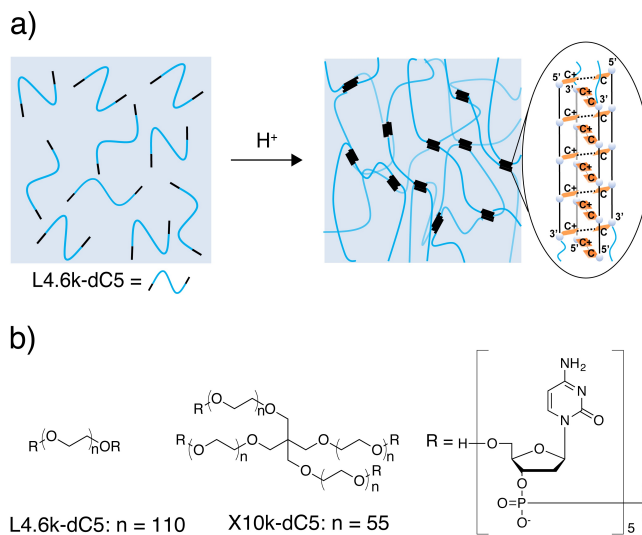L4.6k-dC5: n = 110   X10k-dC5: n = 55

Figure 1. (a) Schematic illustration of present pH responsive hydrogels utilizing i-motif formation. Wavy blue lines represent the PEG segment. Upon the addition of H⁺ to ODN-PEG solution, ODN segments in the conjugates form i-motifs to crosslink PEG segments into a 3D network. (b) Structure of ODN-PEG conjugates used in this study. Five deoxycytidine residues were elongated to each of the ends of $PEG_{4.6k}$ (L4.6k) or 4-arm PEG_{10k} (X10k) using modified HELP.

In this study, we focused on another four-stranded DNA structure. Consecutive deoxycytidine residues are known to form a quite unique quadruplex structure called i-motif,[10] just like deoxyguanosine residues, but in a completely different mechanism. It is composed of an antiparallel pair of parallel two-stranded complexes (Figure 1a). The unit two-stranded complexes consist of consecutive C–protonated-C non-Watson-Crick basepairs, which alternately intercalate to each other to form an i-motif. Protonation of imino-nitrogen of cytosine is essential for the formation of C–protonated-C pairs. Thus, i-motif is only formed under weakly acidic conditions, typically between pH 4.0 and 6.0. As a consequence of complicated modes of complexation, kinetics of i-motif formation is also significantly different from those of G-quadruplexes.[11,12] Typically, association rates for i-motifs are a few orders of magnitude slower than those for G-quadruplexes. Despite above differences in the nature of the quadruplexes, various sophisticated pH-responsive hydrogel systems have been constructed utilizing i-motif to date.[13,14] If ODN-PEG conjugates forming i-motifs prepared by modified HELP turn into hydrogels as dG4-PEG conjugates do, application of pH-responsive hydrogels to bulk material is feasible.

The chemical structures of the conjugates used in this study are presented in Figure 1b. To each of the ends of linear (PEG$_{4.6k}$) or branched (4-arm PEG$_{10k}$) PEG, five consecutive residues of deoxycytidine were coupled in liquid phase using modified HELP, which produces ~10 g of the conjugates in one synthesis with ca. 70% overall yield (see Supporting Information). No special treatment was necessary to synthesize L4.6k-dC5 or X10k-dC5 compared to the syntheses of dG4 conjugates. The X10k-dC5 prepared from 4-arm PEG$_{10k}$ corresponds to simple fusion of two L4.6k-dC5 molecules prepared using PEG$_{4.6k}$ at one carbon atom. The same conjugate concentration in wt% corresponds to the same DNA segment concentration in mM, although the conjugate concentration in mM is in 2:1 ratio for L4.6k-dC5: X10k-dC5.

Figure 2a shows photographs of reversible and pH-responsive sol-gel transitions of 15wt% L4.6k-dC5 solution at room temperature. The initial solution at pH 5.5 immediately turned into hydrogel (i-motif gel) once appropriate amount of 2M HCl solution was added to the solution down to pH 4.5. Addition of another appropriate amount of 2M HCl solution made the system turn into complete fluid at pH 3.5. Addition of aqueous NaOH to this solution again resulted in sol–gel transition. Finally, further addition of aqueous NaOH recovered pH 5.5 solution. The i-motif gel at pH 4.5 stored under room temperature stays in its gel state for more than 6 months to date (data not shown), thus any decomposition of the macromonomers such as deglycosylation of dC5 portion under the acidic gelation conditions is improbable.

Thermal stabilities of the hydrogels were further studied in detail. Temperature-dependent phase diagrams for L4.6k-dC5 and X10k-dC5 over pH, obtained from the inverted test tube method,[15] are shown in Figures 2b and 2c, respectively. The solutions of L4.6k-dC5 showed almost proportionally concentration-dependent phase diagrams with gel-sol transition temperature (T_{sol}) maxima at common pH 4.5. At 10wt%, the solution turns into gel between pH 4.0 and 5.0, and the highest T_{sol} at pH 4.5 is 19°C. For 12wt%, the pH range of gelation is the same with 10wt% solution, although T_{sol} at pH 4.5 rises up to 27°C. The solutions above 15wt% show wider gelation pH range. The 15wt% solution gelates between pH 3.5 and 5.5, whereas

20wt% solution's gelation range is pH 3.0–6.0. T_{sol} for these solutions at pH 4.5 are 35 and 42°C, respectively.

In contrast to the linear conjugate, solutions of X10k-dC5 produce significantly more stable hydrogels (Figure 2c). The solutions of as low as 3wt% form hydrogels between pH 3.5 and 5.5 with T_{sol} at pH 4.5 around 30°C. More concentrated solutions, on the other hand, have far higher T_{sol} maxima. T_{sol} for 5wt% at pH 4.5 is 56°C, and that for 20wt% is even higher than 70°C. The lowest limit of gelation pH is pH 3.0 for 5–20wt%, and the highest limit is pH 6.0 for 5wt% and 6.5 for more concentrated solutions.

These contrastive behaviors between L4.6k-dC5 and X10k-dC5 hydrogels were further confirmed by temperature-dependent rheology measurements of them (Figures 3a and 3b), which gave quite similar T_{sol} values estimated from crossover points to the inverted test tube method (Table S2).
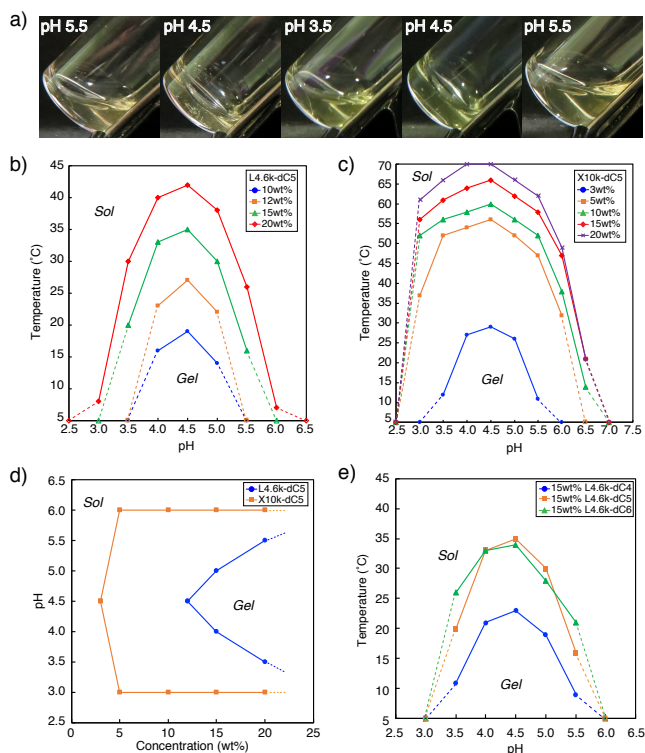

Figure 2. (a) Photographs of reversible pH-responsive gelation of 15wt% L4.6k-dC5 in 0.2 M MES (30 mM NaCl). To adjust pH of the system, appropriate amount of 2 M HCl or 2 M NaOH was added. Boundary between air and sol is horizontal whereas air/hydrogel boundary stays parallel to the bottom of the tubes. (b) Temperature-dependent phase diagrams of 10 (blue circles), 12 (orange squares), 15 (green triangles), and 20wt% (red rhombi) L4.6k-dC5 as a function of solution pH between 2.5 and 6.5. Open symbols represent that no gelation was observed even at 5°C. (c) Temperature-dependent phase diagram of 3 (blue circles), 5 (orange squares), 10 (green triangles), 15 (red rhombi), and 20wt% (purple crosses) X10k-dC5 as a function of solution pH between 2.5 and 7.5. (d) pH-dependent phase diagram of L4.6k-dC5 (blue circles) and X10k-dC5 (orange squares) at 25°C as a function of macromonomer concentration between 0 and 25wt%. Apparent critical gelation concentration is 12wt% for L4.6k-dC5 and 3wt% for X10k-dC5. (e) Temperature-dependent phase diagrams of 15wt% L4.6k-dC4 (blue circles), L4.6k-dC5 (orange squares), and L4.6k-dC6 (green triangles) as a function of solution pH between 2.5 and 6.5.

The phase diagrams in Figure 2d correspond to cross sections of Figure 2b and 2c at 25°C (3D contour charts of them are shown in Figure S2). X10k-dC5 constantly forms hydrogels between pH 3.0 and 6.0 in wide range of concentrations higher than 5wt%. The gelation window of L4.6k-dC5, on the other hand, is quite narrower compared to X10k-dC5. Considering that the thermal stabilities of G-quadruplex gels, in which most of the DNA portions are estimated to form G-quadruplexes, were not very different between L and X series, one possible explanation for the above large differences of T_{sol} for current i-motif gels is relatively low yield of i-motifs in the hydrogels of L4.6k-dC5. Circular dichroism (CD) measurements of the solutions of X10k-dC5 and L4.6k-dC5 (Figure 4a and Table S1), however, showed almost identical formation of i-motifs with typical cotton effects at pH 4.5, and estimated Tm values for them are quite similar to each other (45.5°C for X10k-dC5 at 0.1wt% and 49.0°C for L4.6k-dC5). Taking into account that T_{sol} of L4.6k-dC5 is almost saturated when it is compared with those of L4.6k-dC4 with shorter DNA portions or L4.6k-dC6 (Figure 2e), dC5 portions in both systems completely form i-motifs, and unexpectedly high T_{sol} of X10k-dC5 may be ascribed to the present high concentration of the conjugates ([dC5 portion] > 20 mM), which is one of the advantage of adopting HELP synthesis.

a)   b)
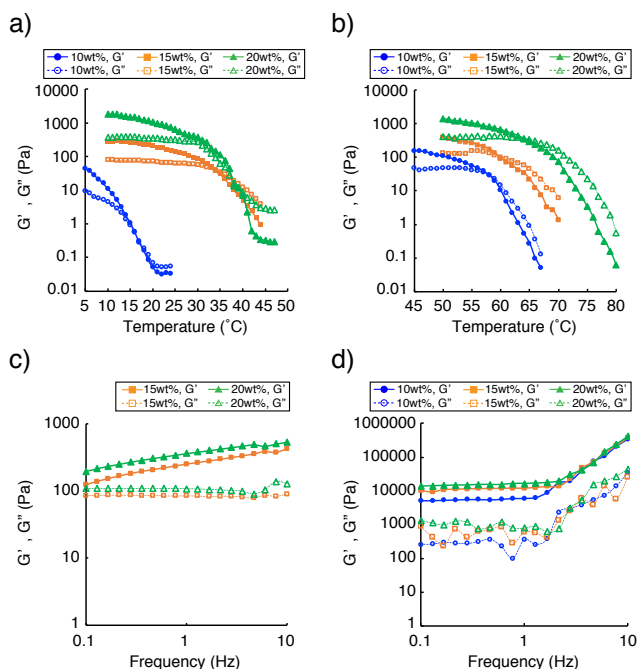

c)   d)

Figure 3. Rheological properties of i-motif gels. (a) Temperature-dependent rheological properties of 10 (blue circles), 15 (orange squares), and 20wt% (green triangles) L4.6k-dC5 hydrogels at pH 4.5 and 0.15 Hz. T_{sol} for 10, 15, 20wt% are 17, 34, and 38°C, respectively. (b) Temperature-dependent rheological properties of 10 (blue circles), 15 (orange squares), and 20wt% (green triangles) X10k-dC5 hydrogels at pH 4.5 and 0.15 Hz. T_{sol} for 10, 15, 20wt% are 58, 60, and 65°C, respectively. (c) Frequency-dependent rheological properties of 15 (orange squares) and 20wt% (green triangles) L4.6k-dC5 hydrogels at pH 4.5 and 25°C. G' is 0.12 kPa for 15wt% and 0.20 kPa for 20wt% at 0.1 Hz. (d) Frequency-dependent rheological properties of 10 (blue circles), 15 (orange squares), and 20wt% (green triangles) X10k-dC5 hydrogels at pH4.5 and 25°C. G' at 0.1 Hz for 10, 15, 20wt% are 5.2, 10, and 13 kPa, respectively.

Rheological measurements at room temperature similarly revealed that X10k-dC5 hydrogels (10–20wt%) are quite stiff along wide range of frequency with the storage moduli (G') around 10 kPa (Figure 3d), which is almost comparable to, or even higher than, that of 10wt% X10k-dG4/K$^+$ hydrogel based on G-quadruplexes, whereas those of 15 and 20wt% L4.6k-dC5 hydrogels are only 0.12 and 0.20 kPa, respectively (Figure 3c). The difference between X10k-dC5 and L4.6k-dC5 systems at the same concentration is only the existence of one chemical linkage in the middle of the PEG portion, and it is known that G' of hydrogels is theoretically proportional to the crosslinking density of the 3D polymer network.[16] The G' values for G-quadruplex gels are indeed 11 kPa for 10wt% X10k-dG4/K$^+$ and 6 kPa for 10wt% L4.6k-dG4/K$^+$. The above large difference of the crosslinking density in i-motif gels, thus, can only be explained by relatively low contribution of i-motifs as crosslinking points compared to G-quadruplexes. Presumably, kinetically fast G-quadruplex formation (association rate for 10wt% L4.6k-dG4/K$^+$ ([dG4 portion] ≈ 40 mM) is calculated to be in ca. 1–10^3 M/s regime, i.e. G-quadruplex formation is completed at least within 10–100 msec time frame)[11] produces more intermolecular complexations than relatively slow i-motif formation (for 10 mM ODN, formation of fully intercalated tetramer takes ca. 1 sec)[12] that allows participations of intramolecular loop structures. The difference of conformation between parallel G-quadruplexes and antiparallel i-motifs in the hydrogels may also contribute to such difference in intermolecular/intramolecular complexation ratio. The fact that the properties of X10k-dC5 hydrogels, in contrast to L4.6k-dC5, match those of X10k-dG4/K$^+$ strongly suggests significant contribution of mechanical connections formed between fused loops in branched PEG. The current X10k-dC5 hydrogels can be another kind of topology-based hydrogel.[17]
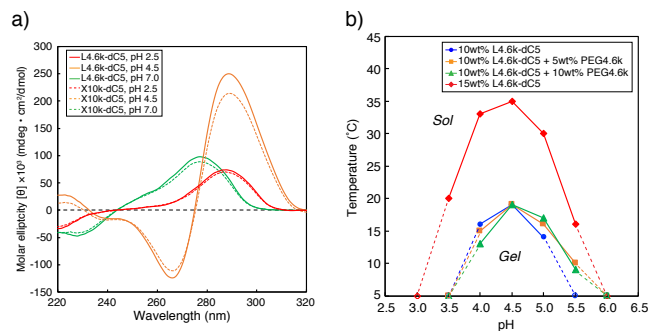
a)   b)

Figure 4. (a) CD spectra of 0.1wt% L4.6k-dC5 (solid lines) and X10k-dC5 (dotted lines) solutions in 0.2 M MES containing 30 mM NaCl at pH 2.5 (red), 4.5 (orange), or 7.0 (green). (b) Temperature-dependent phase diagrams of 10 (blue circles) or 15wt% (red rhombi) L4.6k-dC5 without PEG$_{4.6k}$, or 10wt% L4.6k-dC5 in the presence of 5 (orange squares), or 10wt% PEG$_{4.6k}$ (green triangles) as a function of solution pH between 2.5 and 6.5. Open symbols represent that no gelation was observed even at 5°C.

Another unique feature that distinguishes i-motif gels from G-quadruplex gels is the lack of obvious molecular crowding effect of PEG on hydrogel stabilities.[18] The conjugates used for DNA quadruplex gels contain PEG portion without exception, and they are used in somewhat high concentration around 5–20wt% for gelation. Inherent molecular crowding effect of the PEG portion thus has been expected in the systems. For G-quadruplex gels, addition of extra unmodified PEG indeed significantly stabilized hydrogels. In the current system, on the other hand, addition of extra PEG simply shifted the bell-shape pH profile slightly into neutral region and no significant stabilization was observed (Figure 4b). This change is attributable to

upper shift of apparent pK_a of cytosine, and very similar behavior has been reported for regular i-motifs,[18,19] providing another clear evidence of the contribution of i-motif formation in the gelation.
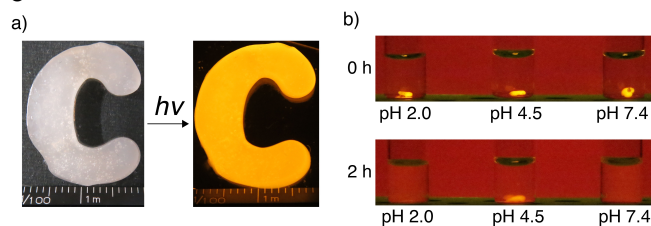

Figure 5. (a) Photographs of 5wt% X10k-dC5 hydrogel (1 g) containing 0.5 µm fluorescent polystyrene beads. The scale on the ruler is 1 mm. (b) pH-responsive guest release from 15wt% X10k-dC5 hydrogel beads (10 µL) containing 0.5 µm fluorescent polystyrene beads. The gel beads prepared by slowly injecting the polymer solution into pH 4.5 MES were immersed in artificial gastric juice (pH 2.0), 0.2 M MES (pH 4.5), or PBS (-) (pH 7.4). After 2 h at room temperature, only the gel bead in pH 4.5 MES remained.

The present i-motif gels can be formed into various shapes containing guests. Figure 5a shows 5wt% X10k-dC5 hydrogel (1 g) containing fluorescent polystyrene beads (d = 0.5 µm) formed in a silicone cooking mold. The scale on the ruler is 1 mm. pH-responsive guest release from 15wt% X10k-dC5 hydrogel beads (10 µL), prepared by slowly injecting the polymer solution containing the polystyrene beads into pH 4.5 MES, was also examined (Figure 5b). This pH corresponds to typical condition of some fruit juice, yogurt, beers, skin surface, or lumen of lysosomes.[20] The hydrogel beads transferred to artificial gastric juice (pH 2.0) or PBS (-) (pH 7.4) rapidly disappeared, and the fluorescent guests were released to the solution (Figure S3). The bead in pH 4.5 MES, quite contrary, still remained even after 2 h at room temperature.

In summary, we have successfully prepared pH responsive DNA quadruplex hydrogel by applying i-motif formation and liquid-phase large scale DNA synthesis. The hydrogels using branched PEG showed unexpectedly high thermal stabilities compared to the *Tm* of the i-motif, as well as high stiffness and high sensitivity to pH change. Introduction of only one chemical linkage between two macromonomers dramatically improved the properties of the hydrogel probably because of topological entanglement. Ease of bulk synthesis and free formation should facilitate the application of current i-motif gels as an additional member of biomaterial used for various medical and healthcare purposes. For example, endosome escape of polysaccharide nanogels from lysosome as DDS carrier has been recently reported.[21] We have preliminarily confirmed that diluted solutions of current dC5-PEG conjugates provide i-motif nanogels in acidic solutions, which will be published elsewhere. Preparation of shape-memory hydrogels,[14] light-driven soft actuators,[22] or controlled drug release matrices used for example on skin, are a few of other feasible applications of the present hydrogels, and the liquid-phase large-scale synthesis should be beneficial for the production of such materials as well.

ASSOCIATED CONTENT

Supporting Information

The Supporting Information is available free of charge on the ACS Publications website.

Experimental details and supplementary data (PDF)

AUTHOR INFORMATION

Corresponding Authors

*E-mail: yohya@kansai-u.ac.jp (Y. Ohya).
*E-mail: kuzuya@kansai-u.ac.jp (A. Kuzuya).

ORCID

Yuichi Ohya: 0000-0002-8862-850X
Akinori Kuzuya: 0000-0003-0003-2996

Author Contributions

§These authors contributed equally.
Notes
The authors declare no competing financial interest.

REFERENCES

(1)   (a) Ahmed, E. M. Hydrogel: Preparation, characterization, and applications: A review. *J. Adv. Res.* **2015**, *6*, 105–121. (b) Hoffman, A. S. Hydrogels for biomedical applications. *Adv. Drug Deliver. Rev.* **2012**, *64*, 18–23. (c) Li, Y.; Rodrigues, J.; Tomás, H. Injectable and biodegradable hydrogels: gelation, biodegradation and biomedical applications. *Chem. Soc. Rev.*, **2012**, *41*, 2193–2221.
(2)   (a) Xiong, X.; Wu, C.; Zhou, C.; Zhu, G.; Chen, Z.; Tan, W. Responsive DNA-Based Hydrogels and Their Applications. *Macromol. Rapid Comm.* **2013**, *34*, 1271–1283. (b) Shao, Y.; Jia, H.; Cao, T.; Liu, D. Supramolecular Hydrogels Based on DNA Self-Assembly. *Acc. Chem. Res.* **2017**, *50*, 659–668. (c) Kahn, J. S.; Hu, Y.; Willner, I. Stimuli-Responsive DNA-Based Hydrogels: From Basic Principles to Applications. *Acc. Chem. Res.* **2017**, *50*, 680–690.
(3)   (a) Adleman, L. M. Molecular Computation of Solutions to Combinatorial Problems *Science* **1994**, *266*, 1021–1024. (b) Seeman, N. C. Nucleic-Acid Junctions and Lattices. *J. Theor. Biol.* **1982**, *99*, 237–247. (c) Komiyama, M.; Yoshimoto, K.; Sisido, M.; Ariga, K. Chemistry Can Make Strict and Fuzzy Controls for Bio-Systems: DNA Nanoarchitectonics and Cell-Macromolecular Nanoarchitectonics. *Bull. Chem. Soc. Jpn.* **2017**, *90*, 967–1004.
(4)   (a) Umeno, D.; Kano, T.; Maeda, M. Affinity Adsorption Separation of Mutagenic Molecules by Polyacrylamide Hydrogels Comprising Double-Stranded DNA. *Anal. Chim. Acta* **1998**, *365*, 101–108. (b) Um, S. H.; Lee, J. B.; Park, N.; Kwon, S. Y.; Umbach, C. C.; Luo, D. Enzyme-Catalysed Assembly of DNA Hydrogel. *Nat. Mater.* **2006**, *5*, 797–801. (c) Liedl, T.; Dietz, H.; Yurke, B.; Simmel, F. Controlled Trapping and Release of Quantum Dots in a DNA-Switchable Hydrogel. *Small* **2007**, *3*, 1688–1693. (d) Qi, H.; Ghodousi, M.; Du, Y.; Grun, C.; Bae, H.; Yin, P.; Khademhosseini, A. DNA-Directed Self-Assembly of Shape-Controlled Hydrogels. *Nat. Commun.* **2013**, *4*, 2275. (e) Song, J.; Im, K.; Hwang, S.; Hur, J.; Nam, J.; Ahn, G.-O.; Hwang, S.; Kim, S.; Park, N. DNA Hydrogel Delivery Vehicle for Light-Triggered and Synergistic Cancer Therapy. *Nanoscale* **2015**, *7*, 9433–9437. (f) Bomboi, F.; Romano, F.; Leo, M.; Fernandez-Castanon, J.; Cerbino, R.; Bellini, T.; Bordi, F.; Filetici, P.; Sciortino, F. Re-Entrant DNA Gels. *Nat*. *Commun*. **2016**, *7*, 13191. (g) Iwasaki, Y.;

Kondo, J.; Kuzuya, A.; Moriyama, R. Crosslinked Duplex DNA Nanogels That Target Specified Proteins. *Sci. Tech. Adv. Mater.* **2016**, *17*, 285–292. (h) Song, P.; Ye, D.; Zuo, X.; Li, J.; Wang, J.; Liu, H.; Hwang, M. T.; Chao, J.; Su, S.; Wang, L.; Shi, J.; Wang, L.; Huang, W.; Lal, R.; Fan, C. DNA Hydrogel with Aptamer-Toehold-Based Recognition, Cloaking, and Decloaking of Circulating Tumor Cells for Live Cell Analysis. *Nano Lett.* **2017**, *17*, 5193-5198.

(5)   (a) Wei, B.; Cheng, I.; Luo, K. Q.; Mi, Y. Capture and Release of Protein by a Reversible DNA-Induced Sol-Gel Transition System. *Angew. Chem. Int. Ed.*, **2008**, *47*, 331–333. (b) Shao, Y.; Li, C.; Zhou, X.; Chen, P.; Yang, Z.; Li, Z.; Liu, D. Responsive Polypeptide-DNA Hydrogel Crosslinked by G-quadruplex. *Acta Chim. Sin.* **2015**, *73*, 815−818. (c) Xiang, B.; He, K.; Zhu, R.; Liu, Z.; Zeng, S.; Huang, Y.; Nie, Z.; Yao, S. Self-Assembled DNA Hydrogel Based on Enzymatically Polymerized DNA for Protein Encapsulation and Enzyme/DNAzyme Hybrid Cascade Reaction. *ACS Appl. Mater. Interfaces*, **2016**, *8*, 22801–22807. (d) Zhang, Z.; Liu, B.; Liu, J. Molecular Imprinting for Substrate Selectivity and Enhanced Activity of Enzyme Mimics. *Small*, **2017**, *13*, 1602730. (e) Zhao, H.; Jiang, G.; Weng, J.; Ma, Q.; Zhang, H.; Ito, Y.; Liu, M. A Signal-Accumulating DNAzyme-Crosslinked Hydrogel for Colorimetric Sensing of Hydrogen Peroxide. *J. Mater. Chem. B*, **2016**, *4*, 4648–4651. (f) Hasuike, E.; Akimoto, A. M.; Kuroda, R.; Matsukawa, K.; Hiruta, Y.; Kanazawa, H.; Yoshida, R. Reversible Conformational Changes in the Parallel Type G-Quadruplex Structure Inside a Thermoresponsive Hydrogel. *Chem. Commun.* **2017**, *53*, 3142–3144. (g) Huang, Y.; Xu, W.; Liu, G.; Tian, L. A Pure DNA Hydrogel with Stable Catalytic Ability Produced by One-Step Rolling Circle Amplification. *Chem. Commun.*, **2017**, *53*, 3038–3041.

(6)   (a) Lu, C.-H.; Qi, X.-J.; Orbach, R.; Yang, H.-H.; Mironi-Harpaz, I.; Seliktar, D.; Willner, I. Switchable Catalytic Acrylamide Hydrogels Cross-Linked by Hemin/G-Quadruplexes. *Nano Lett*, **2013**, *13*, 1298–1302. (b) Kahn, J. S.; Trifonov, A.; Cecconello, A.; Guo, W.; Fan, C.; Willner, I. Integration of Switchable DNA-Based Hydrogels with Surfaces by the Hybridization Chain Reaction. *Nano Lett*, **2015**, *15*, 7773–7778. (c) Lu, C.-H.; Guo, W.; Qi, X.-J.; Neubauer, A.; Paltiel, Y.; Willner, I. Hemin–G-Quadruplex-Crosslinked Poly-N-Isopropylacrylamide Hydrogel: a Catalytic Matrix for the Deposition of Conductive Polyaniline. *Chem. Sci.*, **2015**, *6*, 6659–6664.

(7)   Tanaka, S.; Wakabayashi, K.; Fukushima, K.; Yukami, S.; Maezawa, R.; Takeda, Y.; Tatsumi, K.; Ohya, Y.; Kuzuya, A. Intelligent, Biodegradable, and Self-Healing Hydrogels Utilizing DNA Quadruplexes. *Chem. Asian J.*, **2017**, *12*, 2388–2392.

(8)   Bonora, G. M.; Zaramella, S.; Veronese, F. M. Synthesis by High-Efficiency Liquid-Phase (HELP) Method of Oligonucleotides Conjugated with High-Molecular Weight Poly(ethylene glycol)s (PEGs). *Biol. Proced. Online* **1998**, *1*, 59–69.

(9)   Ellington, E.; Pollard, J. D. Synthesis and Purification of Oligonucleotides. *Curr. Protoc. Mol. Biol.* **2001**, *42*, DOI: 10.1002/0471142727.mb0211s42.

(10)   (a) Gehring, K.; Leroy, J.-L.; Guéron, M. A Tetrameric DNA Structure with Protonated Cytosine-Cytosine Base Pairs. *Nature* **1993**, *363*, 561–565. (b) Xu, B.; Devi, G.; Shao, F. Regulation of Telomeric i-Motif Stability by 5-Methylcytosine and 5-Hydroxymethyl-Cytosine Modification. *Org. Biomol. Chem*. **2015**, *13*, 5646–5651. (c) Garabedian, A.; Butcher, D.; Lippens, J. L.; Miksovska, J.; Chapagain, P. P.; Fabris, D.; Ridgeway, M. E.; Park, M. A.; Fernandez-Lima, F. Structures of the Kinetically Trapped i-Motif DNA Intermediates. *Phys. Chem. Chem. Phys.* **2016**, *18*, 26691–26702.

(11)   Mergny, J.-L.; Cian, A. D.; Ghelab, A.; Saccà, B.; Lacroix, L. Kinetics of Tetramolecular Quadruplexes. *Nucleic Acids Res.* **2005**, *33*, 81–94.

(12)   Leroy, J.-L. The Formation Pathway of i-Motif Tetramers. *Nucleic Acids Res.* **2009**, *37*, 4127–4134.

(13)   (a) Cheng, E.; Xing, Y.; Chen, P.; Yang, Y.; Sun, Y.; Zhou, D.; Xu, L.; Fan, Q.; Liu, D. A pH-Triggered, Fast-Responding DNA Hydrogel. *Angew. Chem. Int. Ed.* **2009**, *48*, 7660–7663. (b) Cheng, E.; Li, Y.; Yang, Z.; Deng Z.; Liu, D. DNA-SWNT Hybrid Hydrogel. *Chem. Commun.* **2011**, *47*, 5545–5547. (c) Guo, W.; Lu, C.-H.; Qi, X.-J.; Orbach, R.; Fadeev, M.; Yang, H.-H.; Willner, I. Switchable Bifunctional Stimuli-Triggered Poly-N-Isopropylacrylamide/DNA Hydrogels. *Angew. Chem. Int. Ed.* **2014**, *53*, 10134–10138.

(14)   (a) Guo, W.; Lu, C.-H.; Orbach, R.; Wang, F.; Qi, X.-J.; Cecconello, A.; Seliktar, D.; Willner, I. pH-Stimulated DNA Hydrogels Exhibiting Shape-Memory Properties. *Adv. Mater.* **2015**, *27*, 73–78. (b) Lu, C.-H.; Guo, W.; Hu, Y.; Qi, X.-J.; Willner, I. Multitriggered Shape-Memory Acrylamide–DNA Hydrogels. *J. Am. Chem. Soc.* **2015**, *137*, 15723–15731. (c) Hu, Y.; Kahn, J. S.; Guo, W.; Huang, F.; Fadeev, M.; Harries, D.; Willner, I. Reversible Modulation of DNA-Based Hydrogel Shapes by Internal Stress Interactions. *J. Am. Chem. Soc.* **2016**, *138*, 16112–16119.

(15)   Nguyen, M. K.; Lee, D. S. Oligo(amidoamine)s Hydrogels with Tunable Gel Properties. *Chem. Commun.* **2010**, *46*, 3583–3585.

(16)   Jiang, H.; Su, W.; Mather, P. T.; Bunning, T. J. Rheology of Highly Swollen Chitosan/Polyacrylate Hydrogels. *Polymer* **1999**, *40*, 4593–4602.

(17)   Noda, Y.; Hayashi, Y; Ito, K. From Topological Gels to Slide-Ring Materials. *J. Appl. Polym. Sci.* **2014**, *131*, 40509.

(18)   Nakano, S.; Miyoshi, D.; Sugimoto, N. Effects of Molecular Crowding on the Structures, Interactions, and Functions of Nucleic Acids. *Chem. Rev.* **2014**, *114*, 2733–2758.

(19)   (a) Zhao, C.; Ren, J.; Qu, X. Single-Walled Carbon Nanotubes Binding to Human Telomeric i-Motif DNA Under Molecular-Crowding Conditions: More Water Molecules Released. *Chem. Eur. J*, **2008**, *14*, 5435–5439. (b) Rajendran, A.; Nakano, S.-I.; Sugimoto, N. Molecular Crowding of the Cosolutes Induces an Intramolecular i-Motif Structure of Triplet Repeat DNA Oligomers at Neutral pH. *Chem. Commun.* **2010**, *46*, 1299–1303. (c) Cui, J.; Waltman, P.; Le, V.; Lewis, E. The Effect of Molecular Crowding on the Stability of Human c-MYC Promoter Sequence I-Motif at Neutral pH. *Molecules*, **2013**, *18*, 12751–12767.

(20)   Mindell, J. A. Lysosomal Acidification Mechanisms. *Annu. Rev. Physiol.* **2012**, *74*, 69–86.

(21)   Toita, S.; Sawada, S.; Akiyoshi, K. Polysaccharide Nanogel Gene Delivery System with Endosome-Escaping Function: Co-Delivery of Plasmid DNA and Phospholipase A2. *J. Control. Release* **2011**, *155*, 54–59.

(22)   Liu, H.; Xu, Y.; Li, F.; Yang, Y.; Wang, W.; Song, Y.; Liu, D. Light-Driven Conformational Switch of i-Motif DNA. *Angew. Chem. Int. Ed.* **2007**, *46*, 2515–2517.